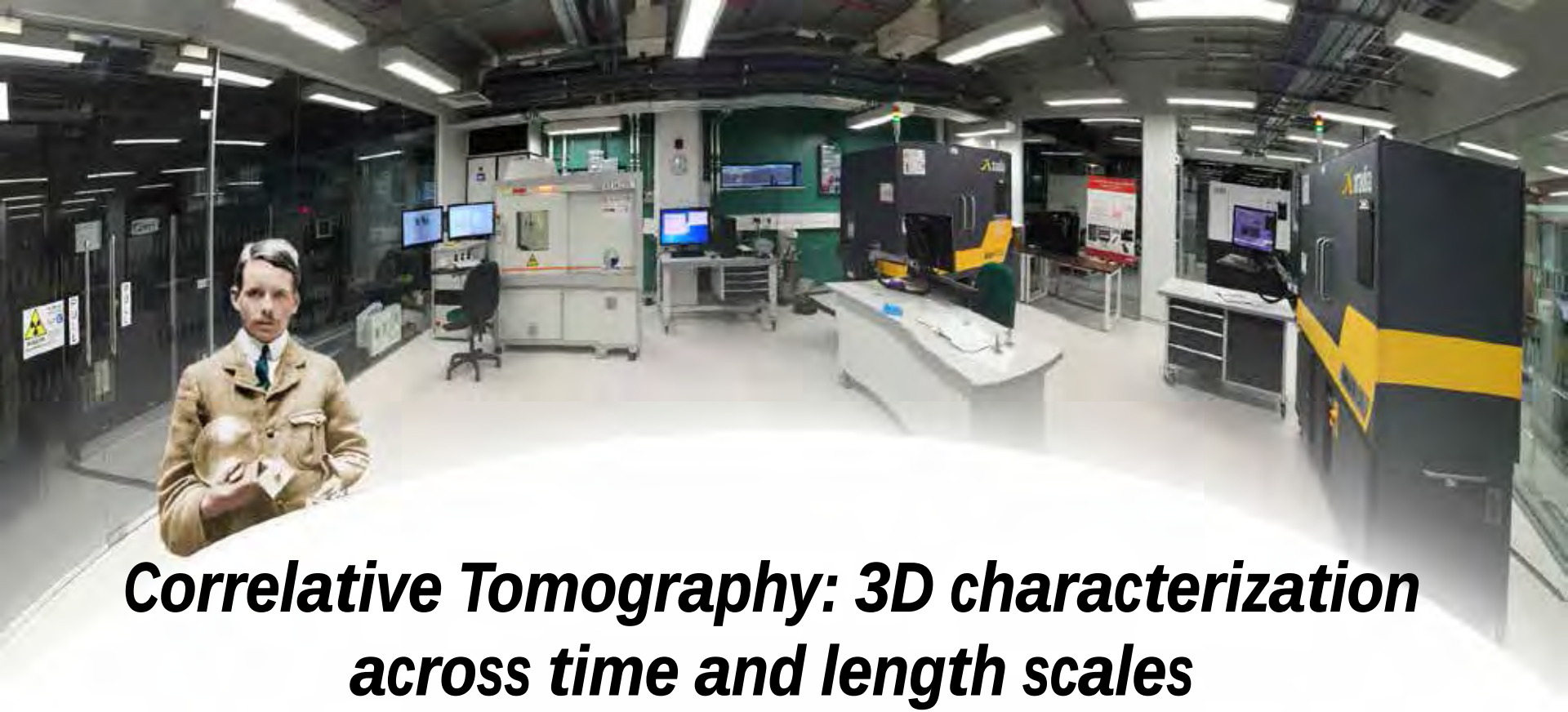

Correlative Tomography: 3D characterization across time and length scales

Dr Tim Burnett

Henry Moseley X-ray Imaging Facility, School of Materials, The University of Manchester, Manchester, UK

MANCHESTER 1824
The University of Manchester

manchester X-Ray Imaging Facility

MANCHESTER 1824
The University of Manchester

Overview

- Introduction to X-ray CT and FIB-SEM serial sectioning
- Clever characterization techniques
- Correlative Tomography

- Website now has all scanners and rigs listed with specs: http://www.mxif.manchester.ac.uk/

X-ray Computed Tomography (CT)

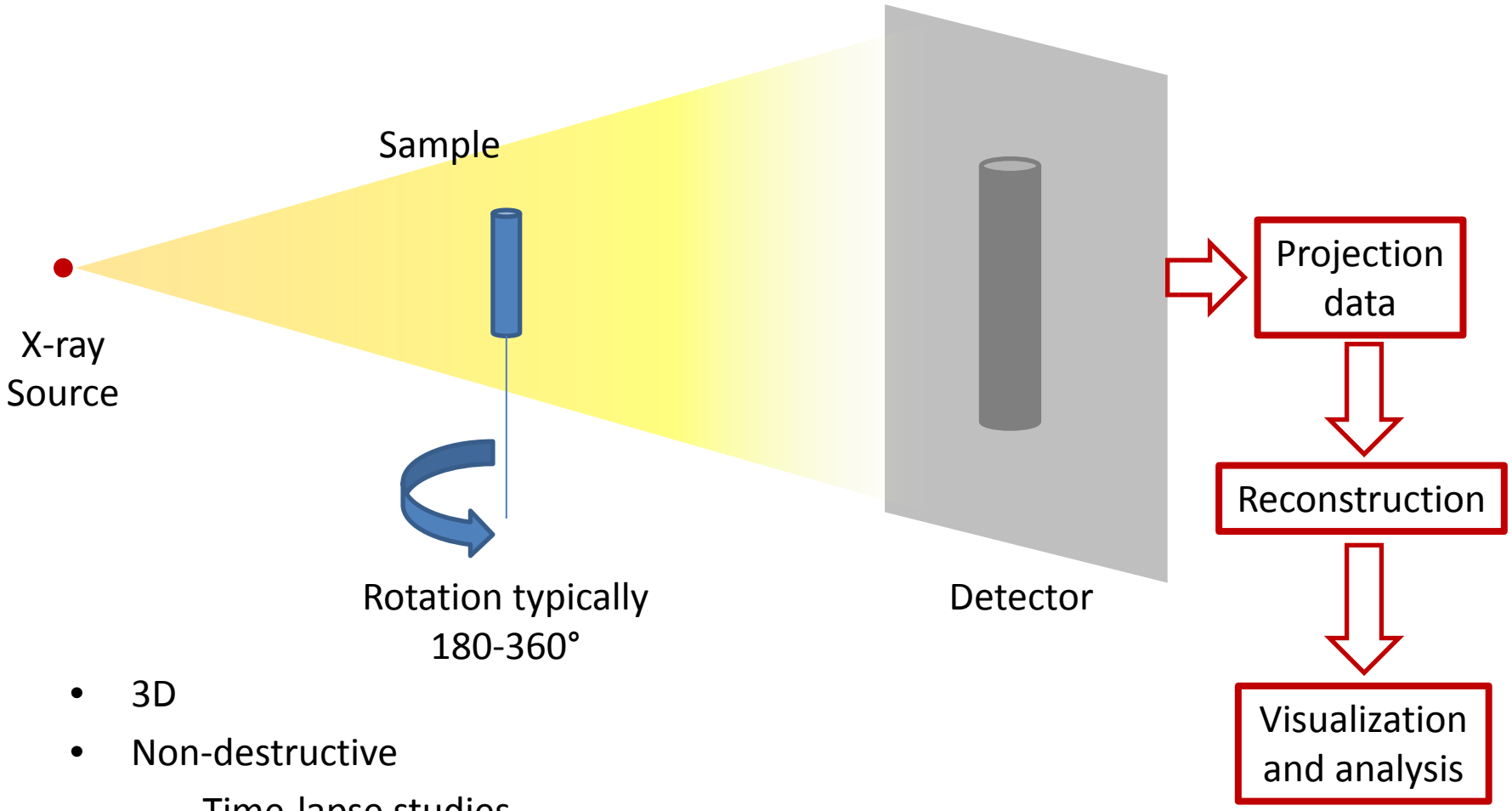

- 3D
- Non-destructive
  - Time-lapse studies
  - Correlative tomography
- Multiscale
- Absorption imaging only gives electron density contrast

FIB-SEM serial sectioning

~15 cm

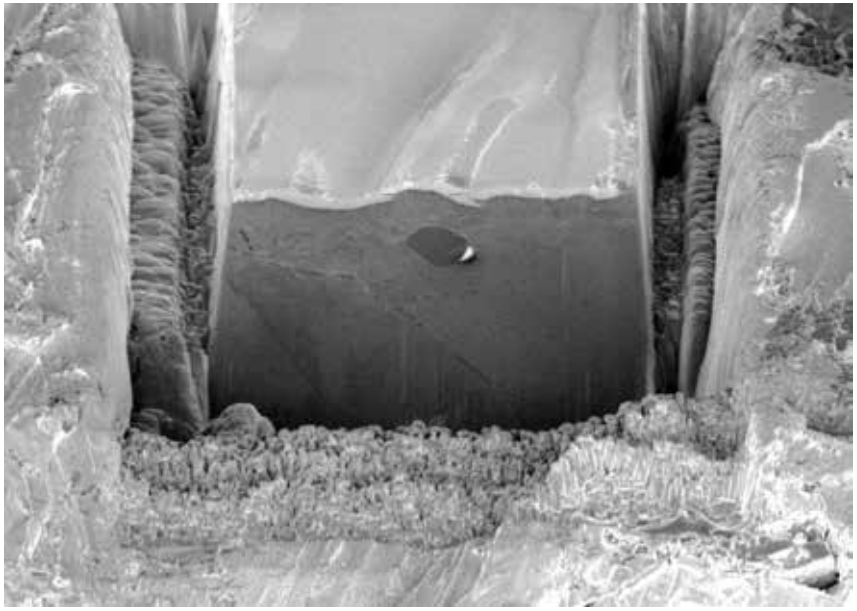

15 µm

- 3D
- Nanoscale resolution
- Rich microstructural contrast- can be combined with EDX and EBSD
- Multiscale
- Destructive!

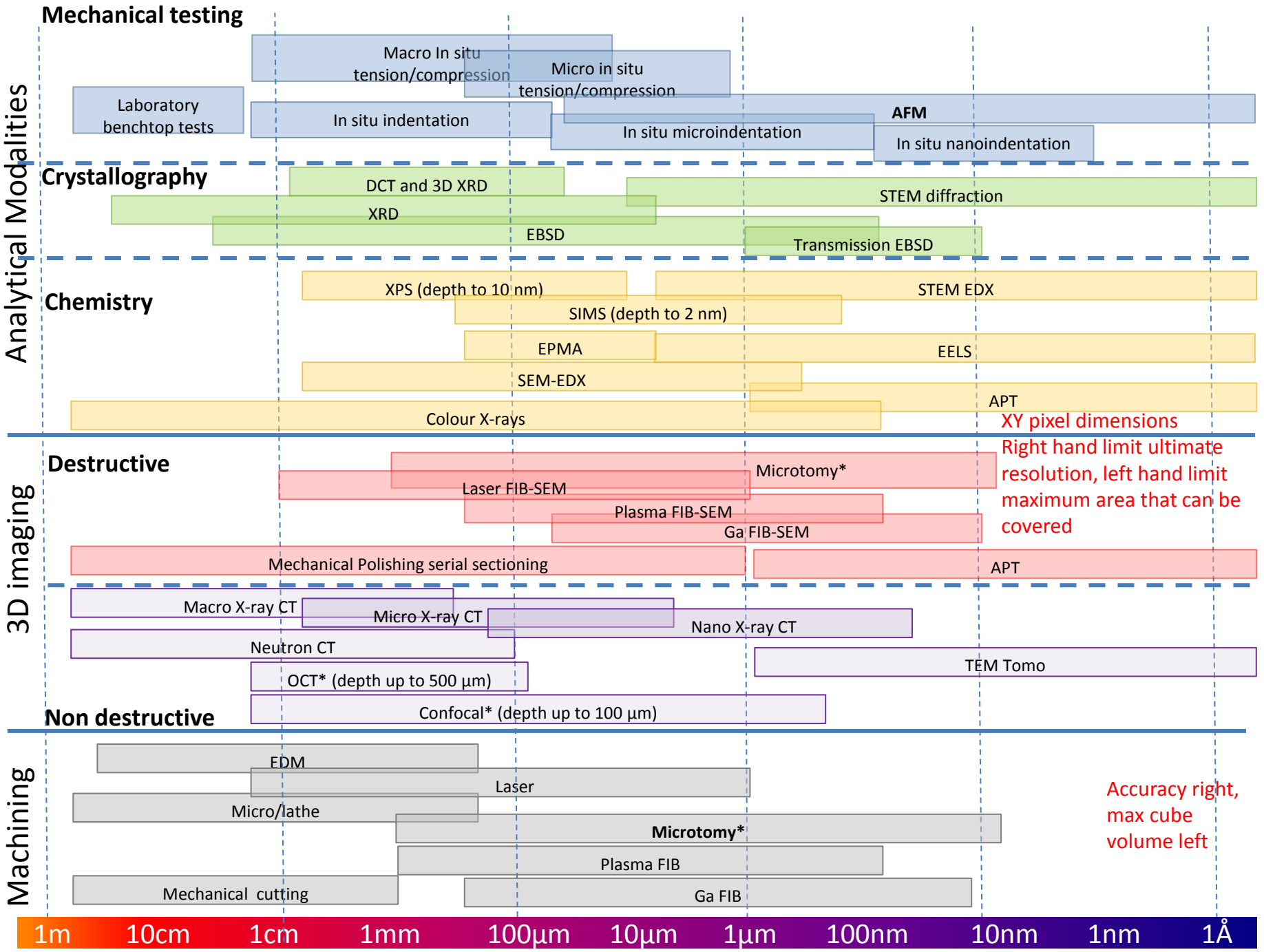
Analytical Modalities
Mechanical testing
Macro In situ tension/compression
Micro in situ tension/compression
Laboratory benchtop tests
In situ indentation
In situ microindentation
AFM
In situ nanoindentation
Crystallography
DCT and 3D XRD
STEM diffraction
XRD
EBSD
Transmission EBSD
Chemistry
XPS (depth to 10 nm)
STEM EDX
SIMS (depth to 2 nm)
EPMA
EELS
SEM-EDX
APT
Colour X-rays
XY pixel dimensions
Right hand limit ultimate resolution, left hand limit maximum area that can be covered
3D imaging
Destructive
Microtomy*
Laser FIB-SEM
Plasma FIB-SEM
Ga FIB-SEM
Mechanical Polishing serial sectioning
APT
Macro X-ray CT
Micro X-ray CT
Nano X-ray CT
Neutron CT
TEM Tomo
OCT* (depth up to 500 µm)
Non destructive
Confocal* (depth up to 100 µm)
Machining
EDM
Laser
Micro/lathe
Microtomy*
Plasma FIB
Mechanical cutting
Ga FIB
Accuracy right, max cube volume left
1m
10cm
1cm
1mm
100µm
10µm
1µm
100nm
10nm
1nm
1Å

Effect of punch shape on flow

- 0.5mm glass beads within a 20mm diameter die
- Displacement fields mapped using digital image correlation

sub-volume size
= 1.1mm x 1.1mm x 1.1mm

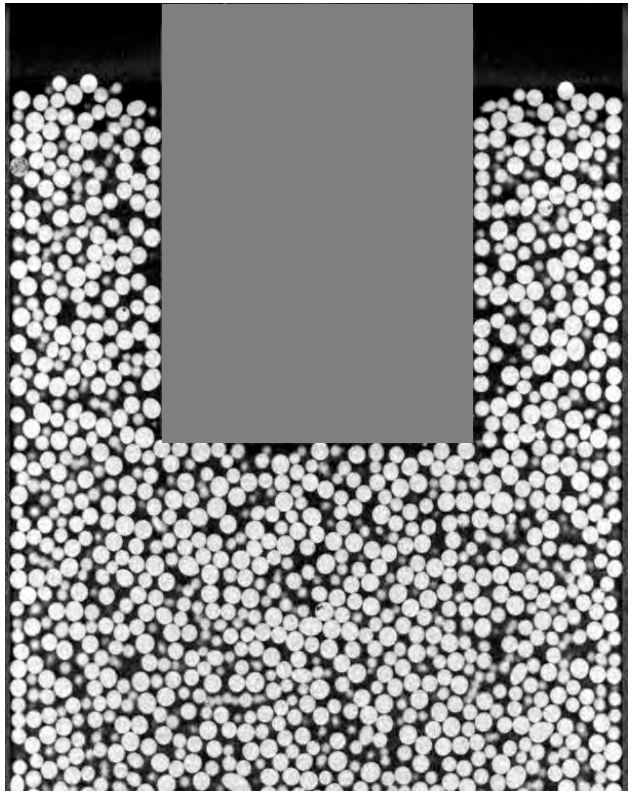

Flat Punch

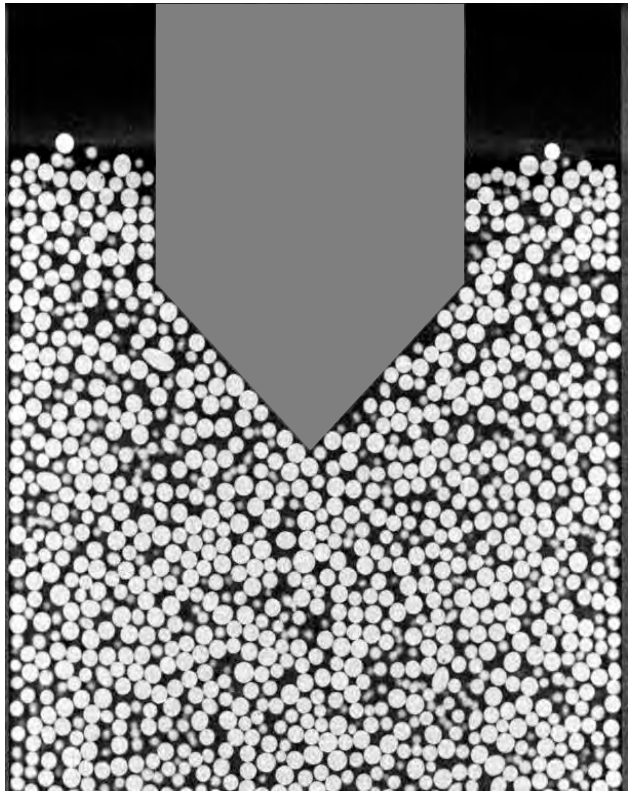

Angled Punch

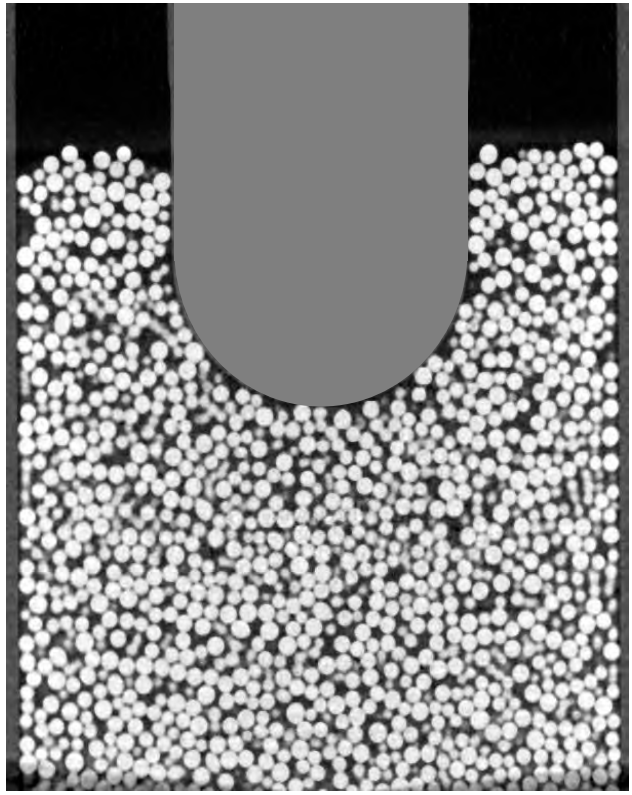

Rounded Punch

Work by Sam McDonald- UoM

Comparison of displacements

- Flat and angled punches show most significant differences
  - Displacement magnitudes and flow characteristics, for the same punch displacement
- Rounded punch shows similarities between the two
  - Hairpin trajectory as with flat punch; particles pushed laterally as with angled punch

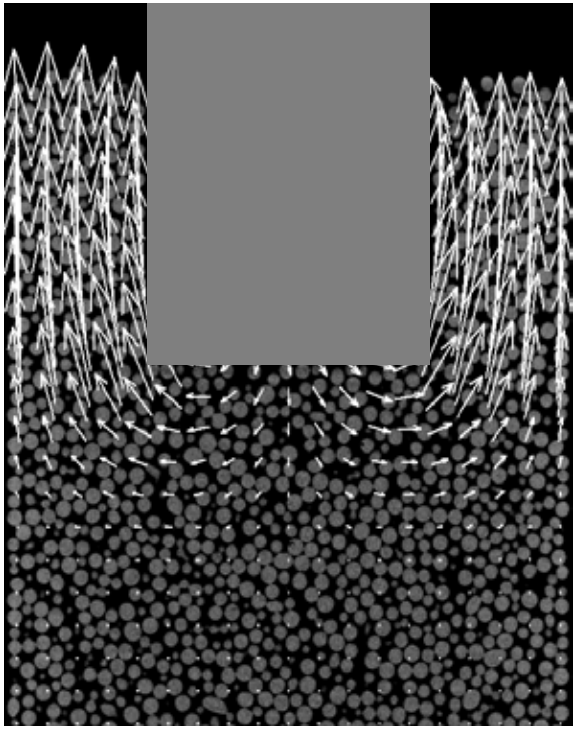

Flat punch

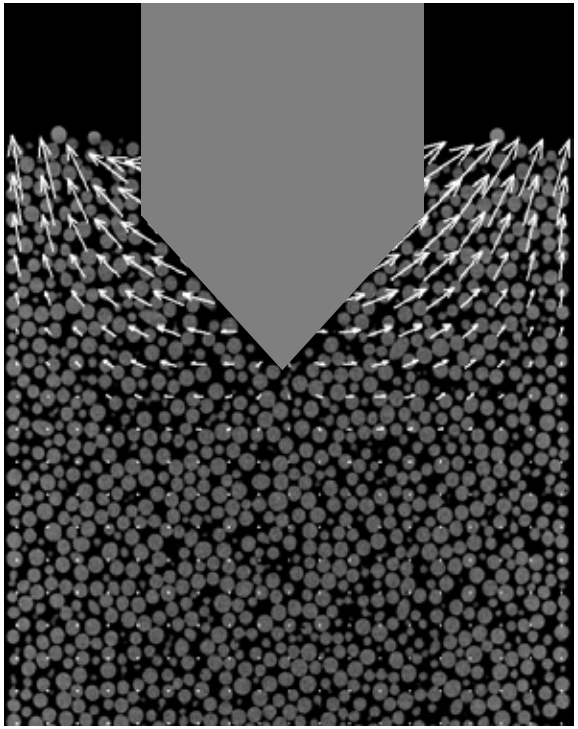

Angled punch

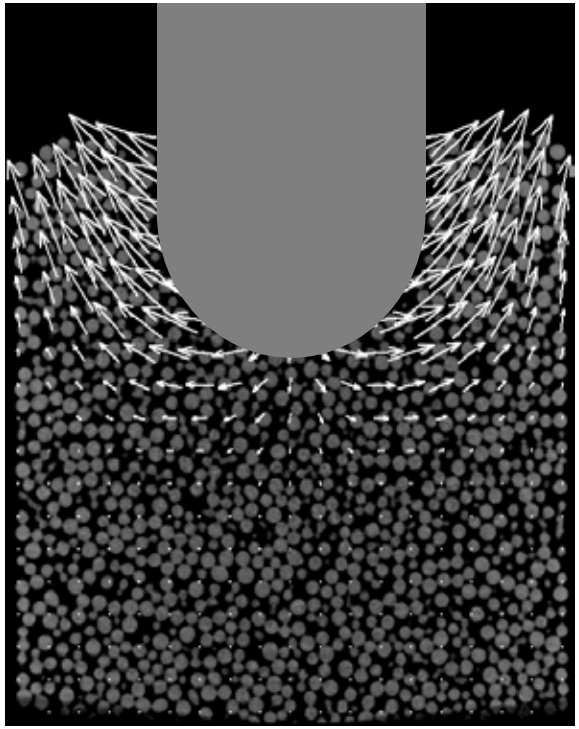

Rounded punch

Work by Sam McDonald- UoM

Axial strain fields

- Axial strains of 10% in compression underneath flat and rounded punches; only 2% underneath tip of angled punch
  - Consistent with redistribution of particles observed from vector displacements
- Axial strains of 60% adjacent to corners of flat punch; significantly higher than for angled (20%) or rounded (35%) punches

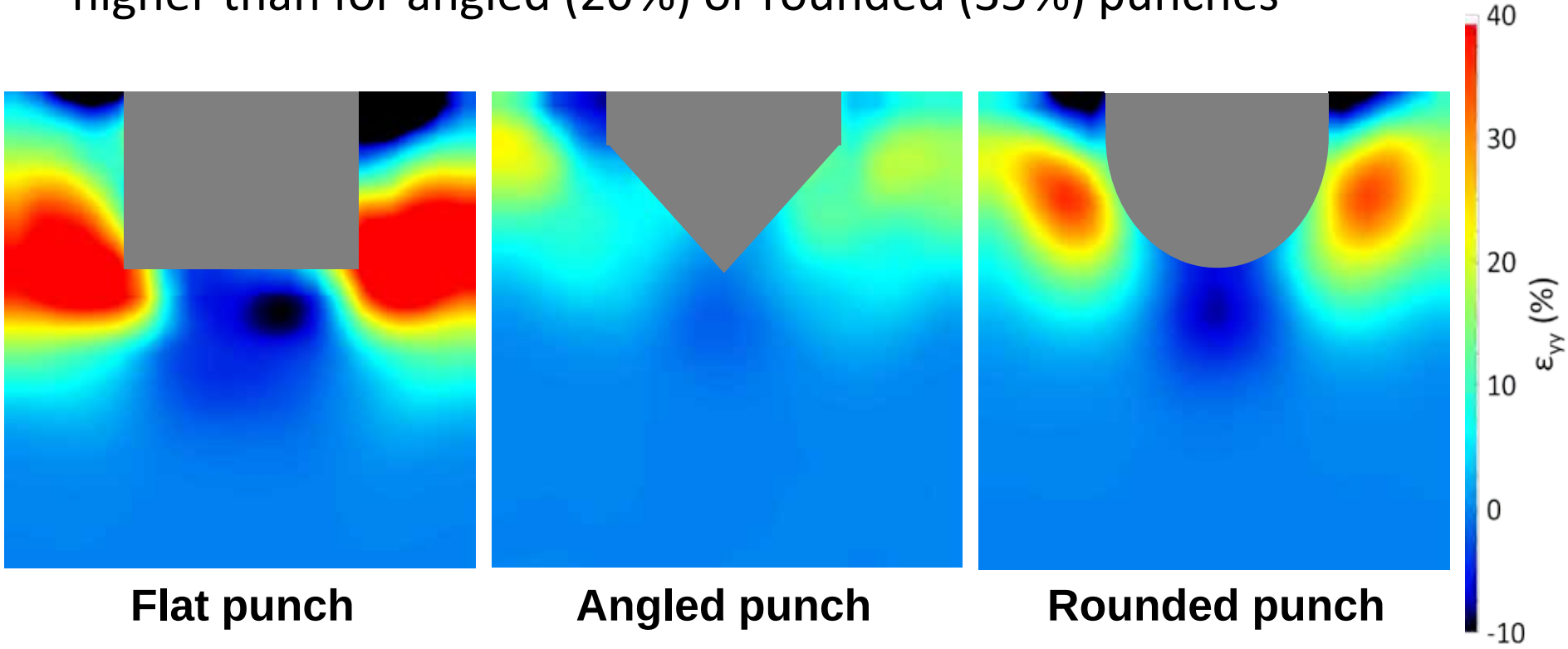

Flat punch **Angled punch** **Rounded punch**

Work by Sam McDonald- UoM

Powder movement during sintering

- Can use digital image correlation to determine collective particle movements with time

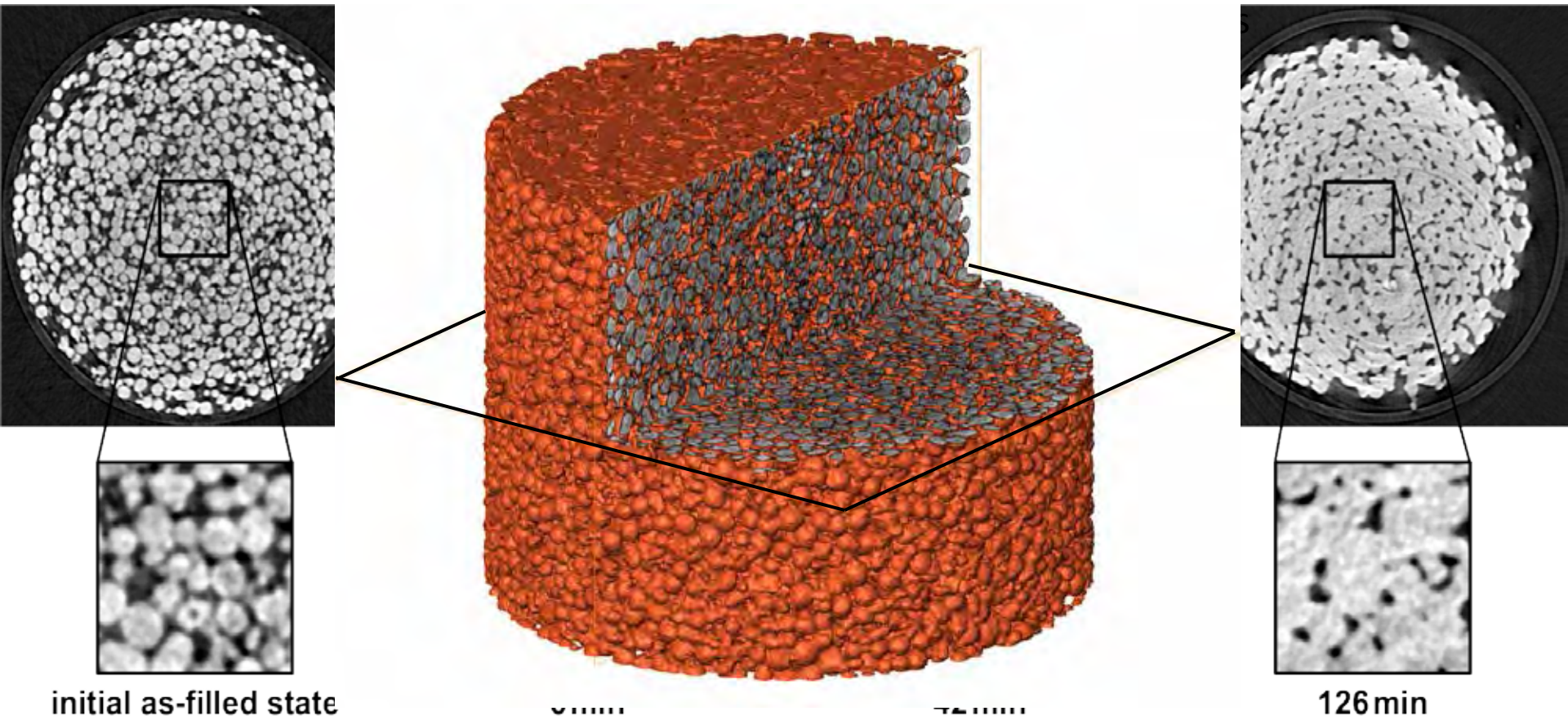

Work by Sam McDonald- UoM

Powder movement during sintering

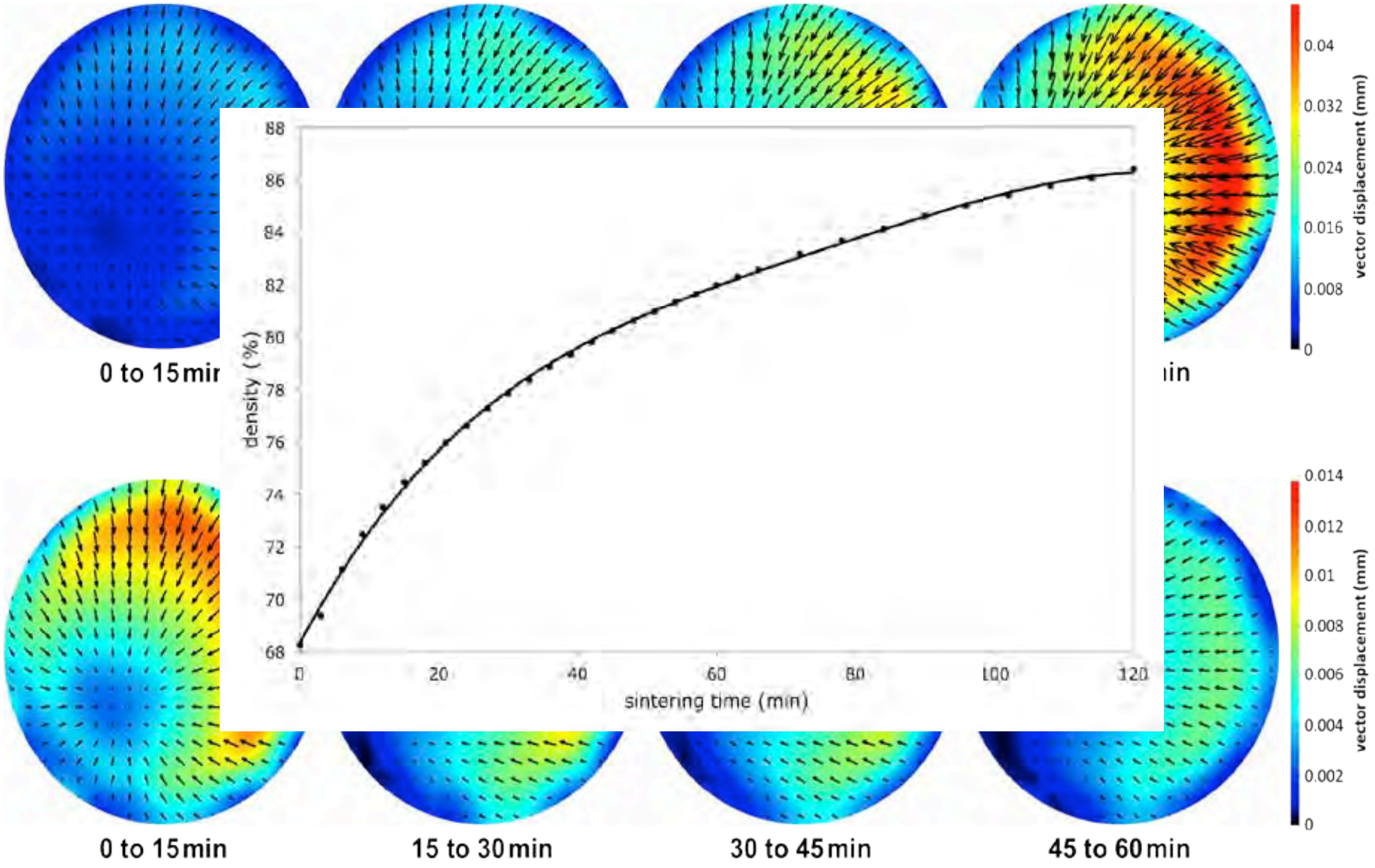

Work by Sam McDonald- UoM

Time lapse indentation on dentin using nanoCT

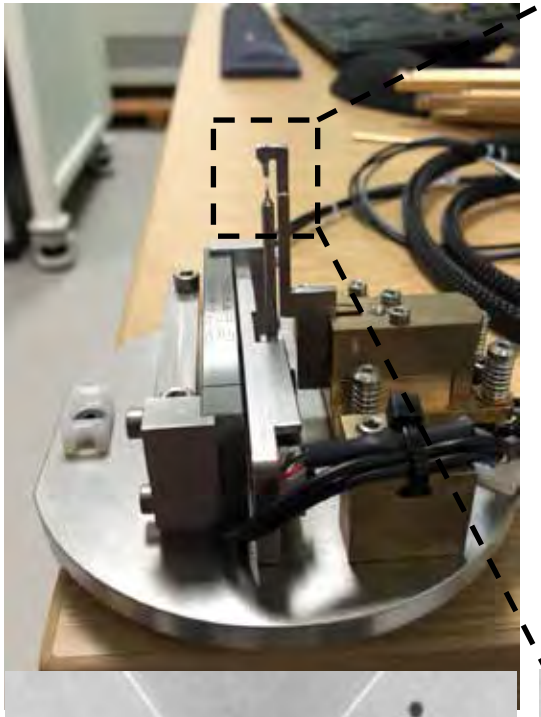

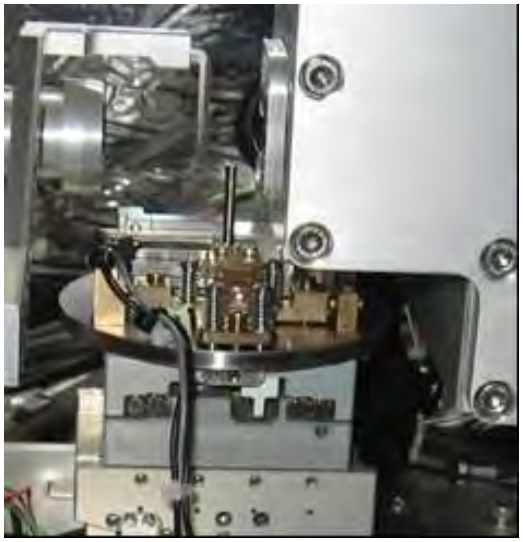

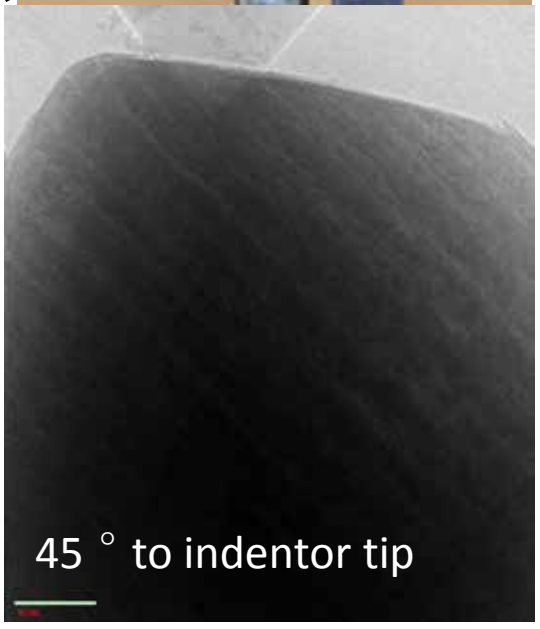

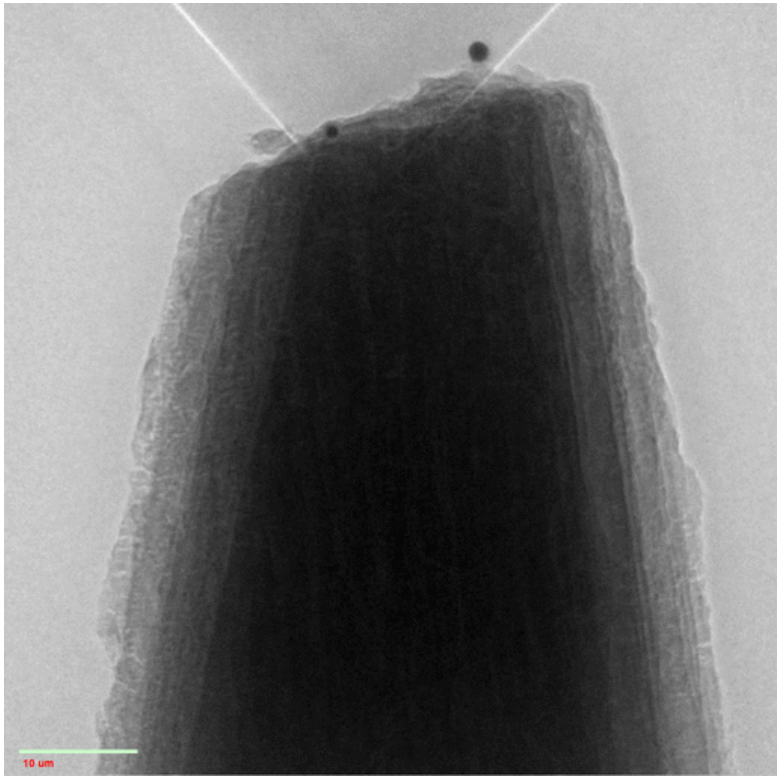

Work by Rob Bradley-UoM

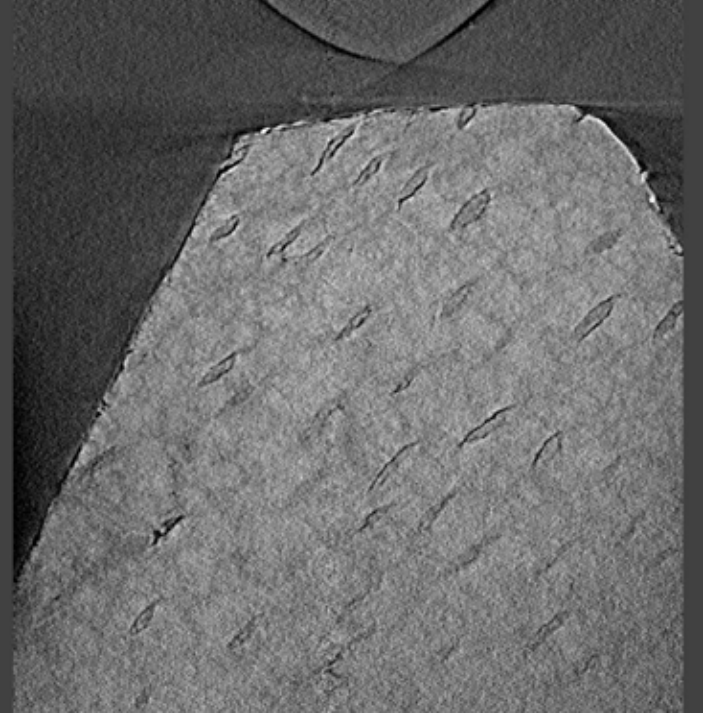

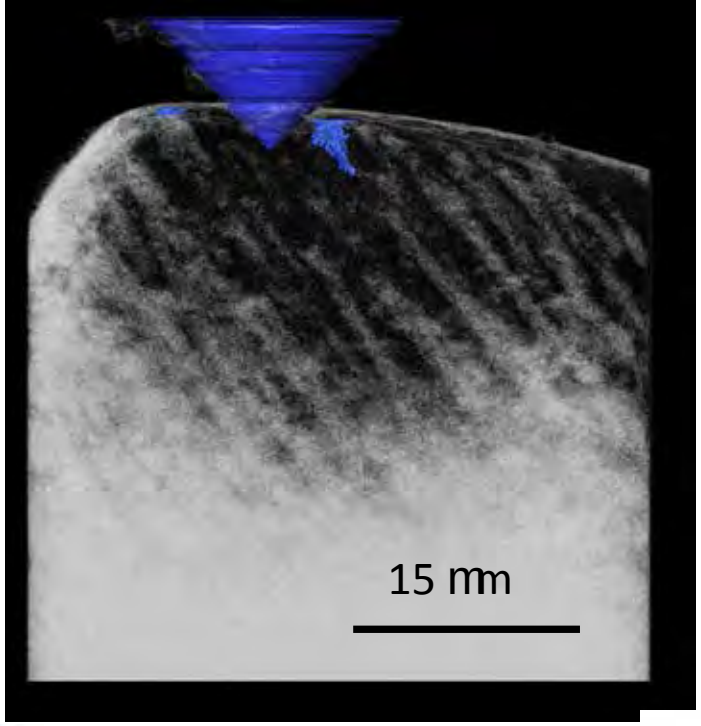

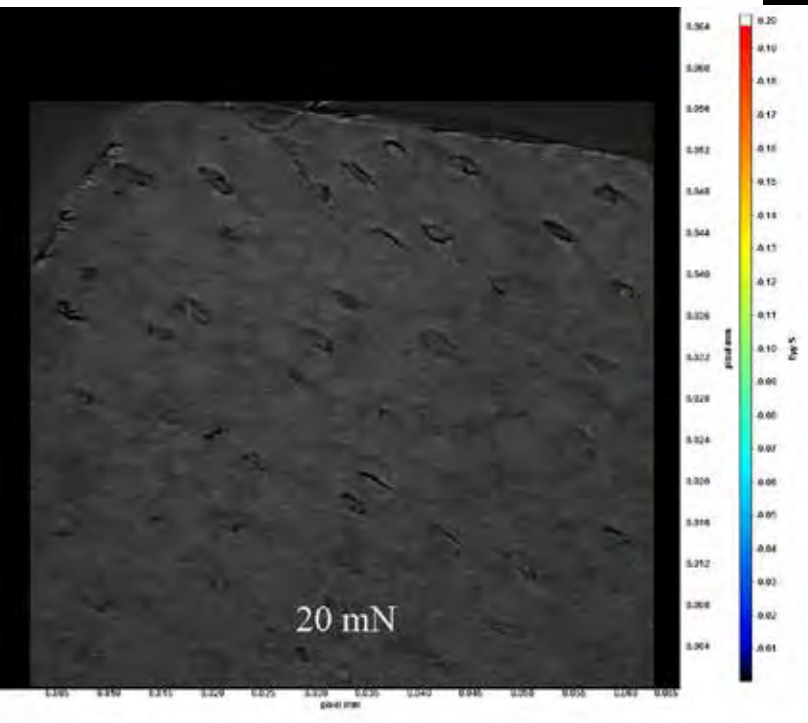

45 ° to the indentor

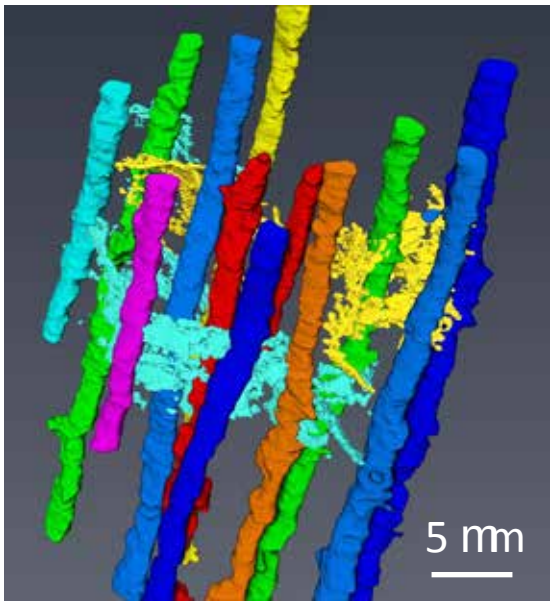

Parallel to the indentor

5 mm

LabDCT reconstruction

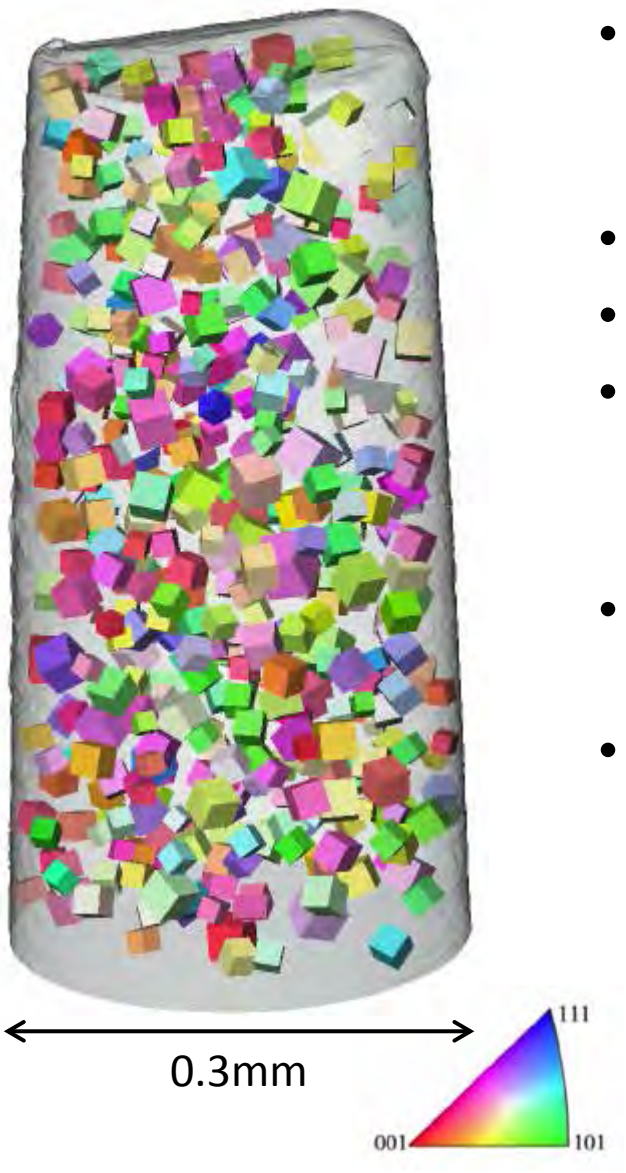

- Measurements performed on a ZEISS Xradia 520 Versa X-ray microscope with DCT modality
- 70 kV, 86 µA; S-S, S-D distances = 12mm
- Effective pixel size = 1.7µm
- Reconstruction using GrainMapper3D analysis package from Xnovo Technology

- Reconstructed grain map of titanium alloy sample (Ti-β21S)
- Output:-
  - Grain centroid position
  - Grain volume
  - Crystallographic orientation

Work by Sam McDonald- UoM

Validation of grain orientations

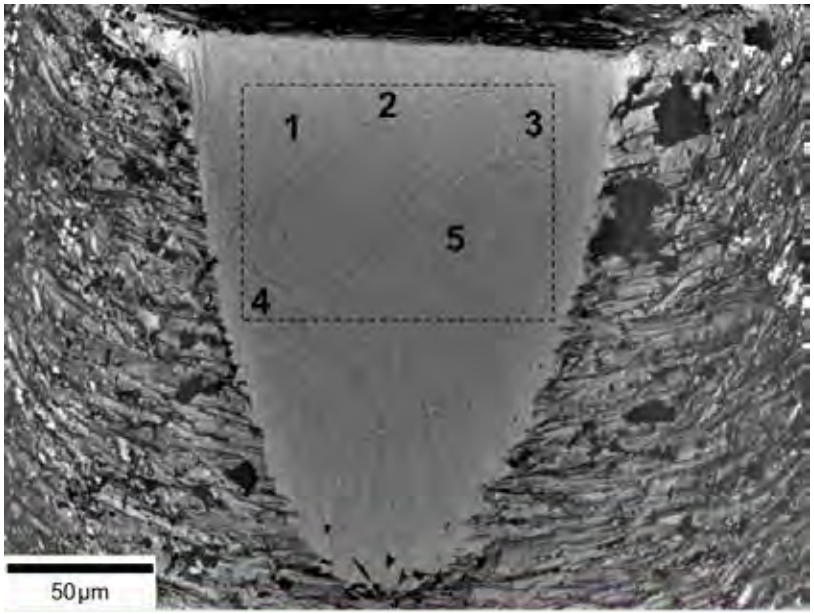

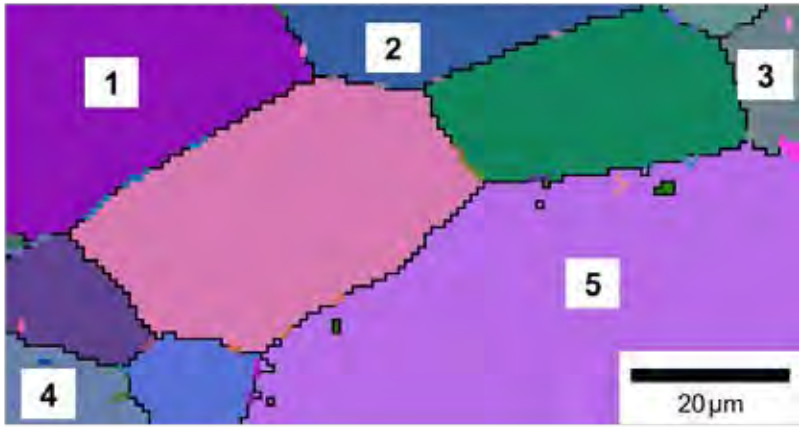

EBSD map of region indicated

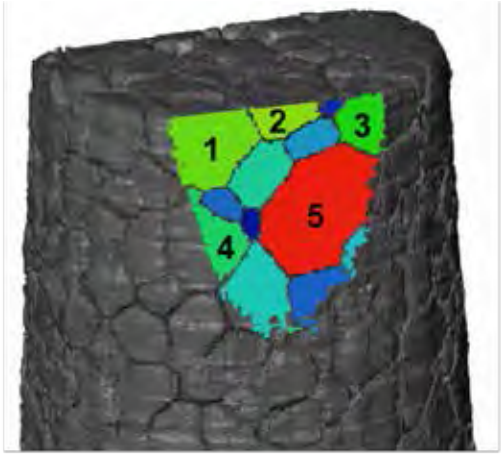

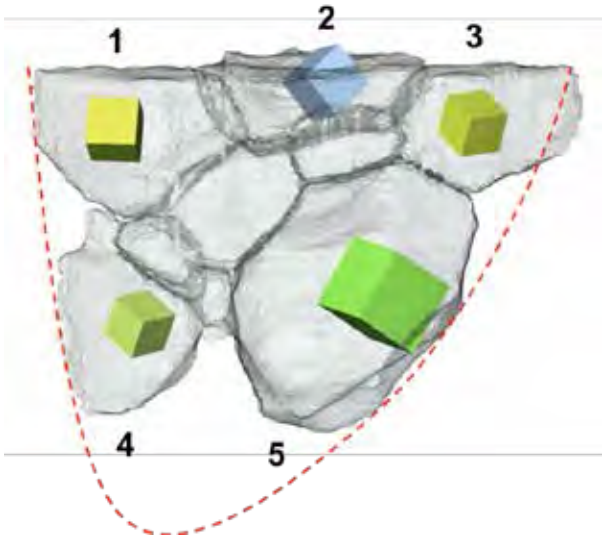

Individual grains 1–5 with corresponding matched grains from lab-DCT (cubes)

Work by Sam McDonald- UoM

Hyperspectral CT (Lab-based)

Mic
X-r

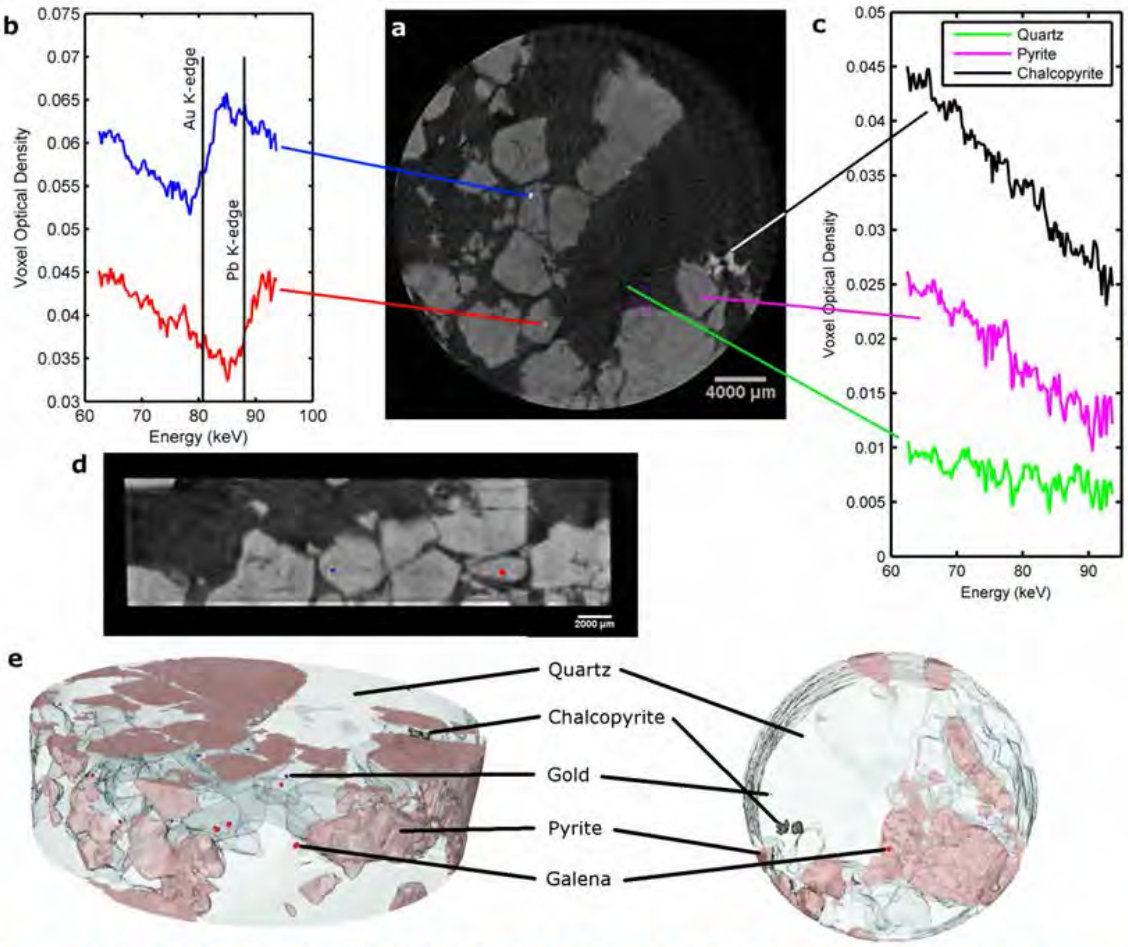

Figure 3: 3D distribution of mineral phases in a mineralised ore sample from a gold-rich hydrothermal vein. (a) Grayscale tomographic slice through the sample created by integrating over the full spectral range. (b) Voxel spectra showing Au and Pb K-edges. (c) Voxel spectra from quartz, pyrite and chalcopyrite minerals. (d) Vertical slice through the sample with Au (blue) and Pb (red) containing voxels segmented and coloured. (e) 3D visualisations of the distribution of mineral phases in the sample.

ris Egan- UoM

XRD-CT (synchrotron based)

- Suitable for in situ operando studies

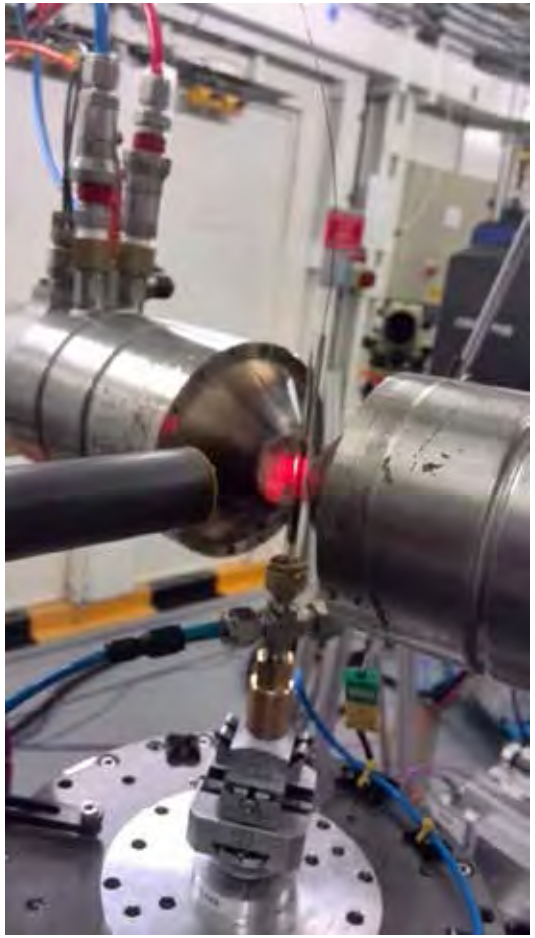

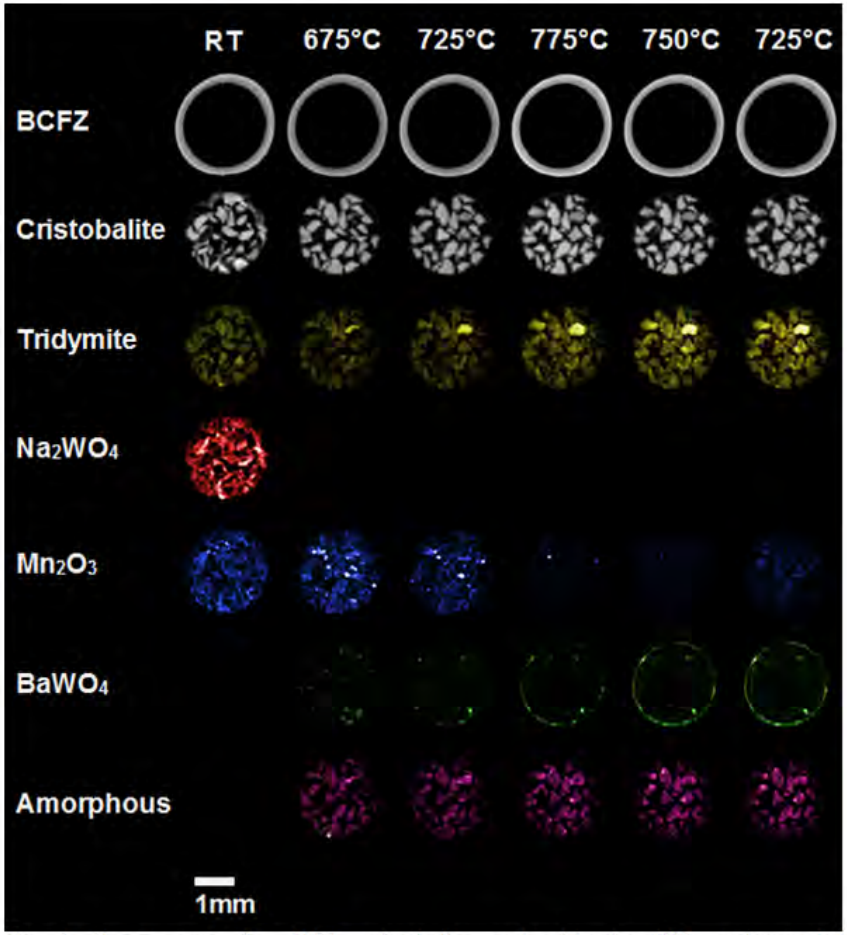

Fig. 2 Phase maps for BCFZ, cristobalite and tridymite (SiO_2 polymorphs), Na_2WO_4, Mn_2O_3, Ba_2WO_4 and an amorphous phase as determined from the XRD-CT data. These maps have been obtained from the integrated intensities of the respective phases. The relative change of each component, as determined from the integrated intensities (for the whole sample slice), is shown in Figure S4.

Work by Simon Jacques and Chris Egan- UoM

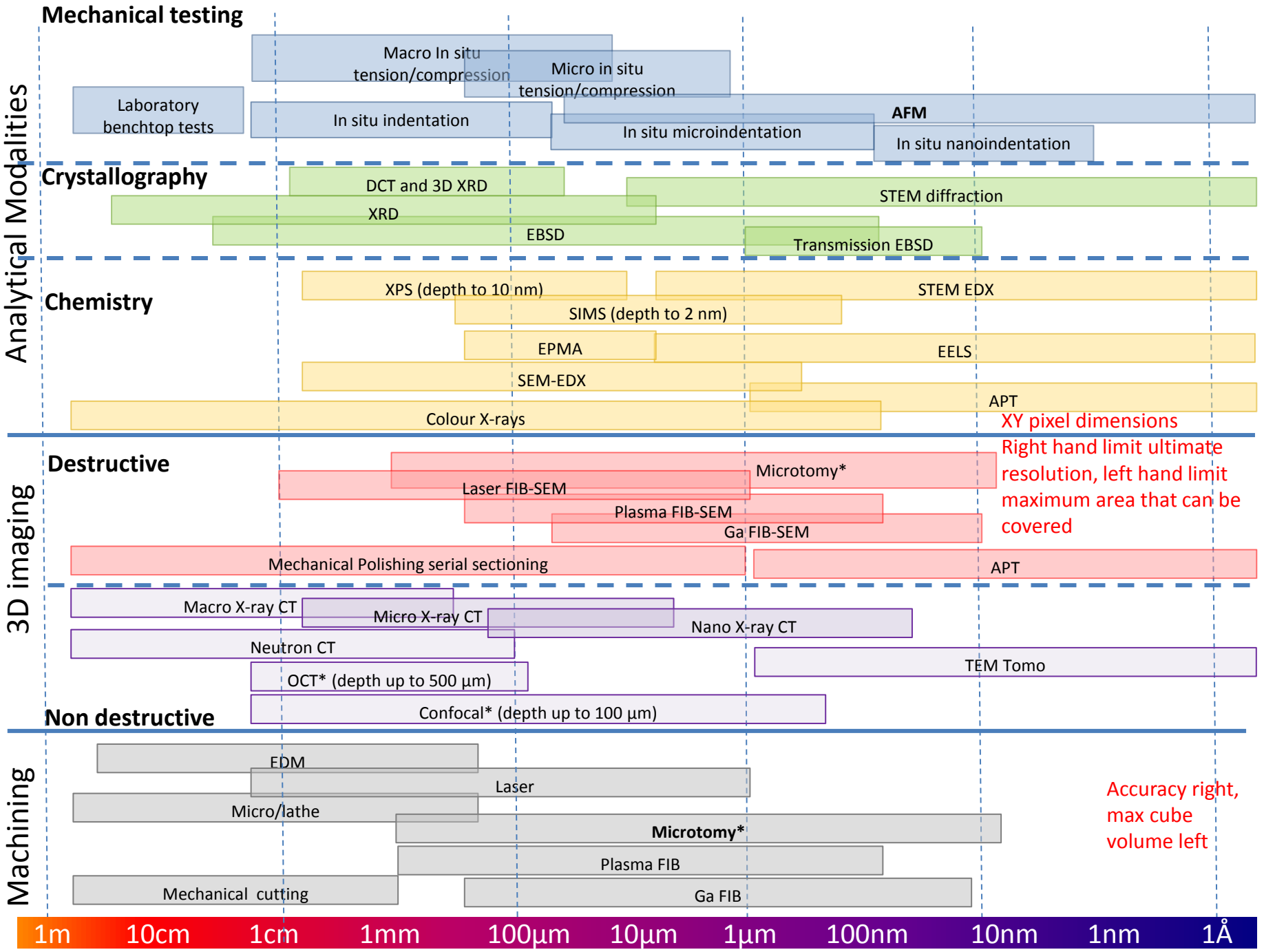
Analytical Modalities
Mechanical testing
Macro In situ tension/compression
Micro in situ tension/compression
Laboratory benchtop tests
In situ indentation
In situ microindentation
AFM
In situ nanoindentation
Crystallography
DCT and 3D XRD
STEM diffraction
XRD
EBSD
Transmission EBSD
Chemistry
XPS (depth to 10 nm)
STEM EDX
SIMS (depth to 2 nm)
EPMA
EELS
SEM-EDX
APT
Colour X-rays
XY pixel dimensions
Right hand limit ultimate resolution, left hand limit maximum area that can be covered
3D imaging
Destructive
Microtomy*
Laser FIB-SEM
Plasma FIB-SEM
Ga FIB-SEM
Mechanical Polishing serial sectioning
APT
Macro X-ray CT
Micro X-ray CT
Nano X-ray CT
Neutron CT
TEM Tomo
OCT* (depth up to 500 µm)
Non destructive
Confocal* (depth up to 100 µm)
Machining
EDM
Laser
Micro/lathe
Microtomy*
Plasma FIB
Mechanical cutting
Ga FIB
Accuracy right, max cube volume left
1m
10cm
1cm
1mm
100µm
10µm
1µm
100nm
10nm
1nm
1Å

Connecting timescales: Macroscale X-ray CT

Sample immersed in Chloride Solution and polarized

- Time lapse images show nucleation and growth of corrosion pits
- Identification of the fastest or slowest growing pits

But we need to better characterize the pit morphology….

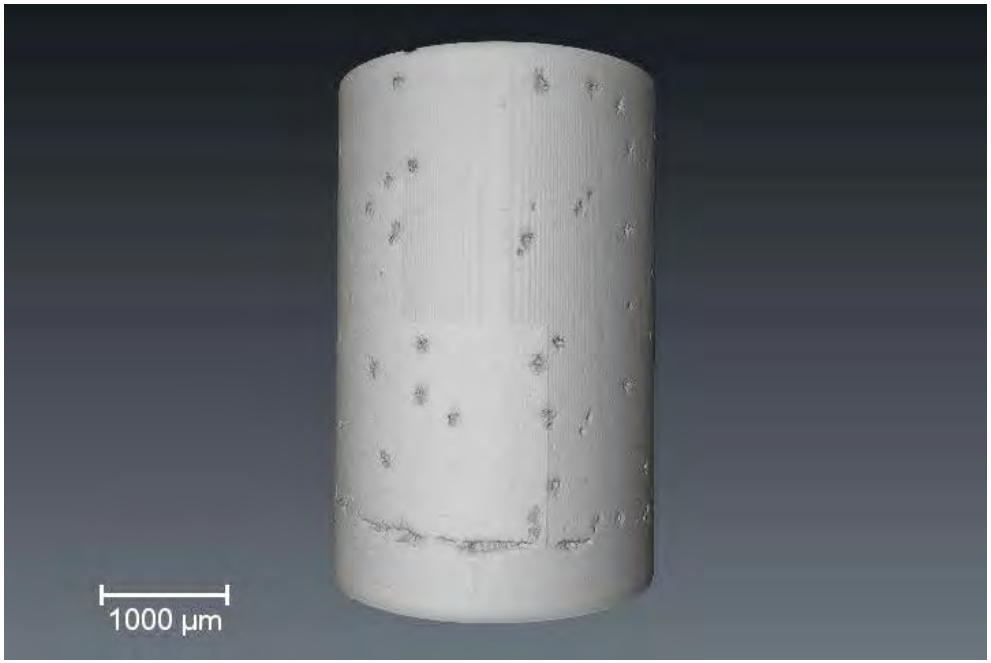

Connecting Scales: high-resolution X-ray CT

Use macroscale X-ray CT as a 3D map to find RoI for microscale X-ray CT

- We can now see the detailed morphology of the corrosion pit, revealing a network of ‘intergranular’ corrosion surrounding the pit

We now need to explore the microstructure around the pit in more detail….

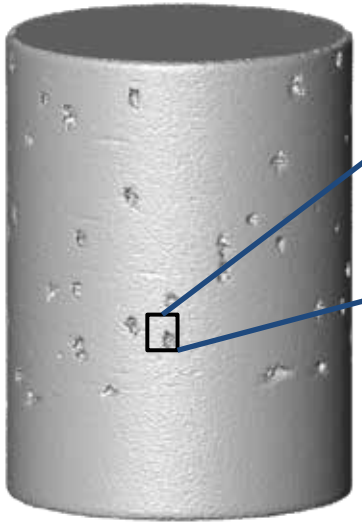

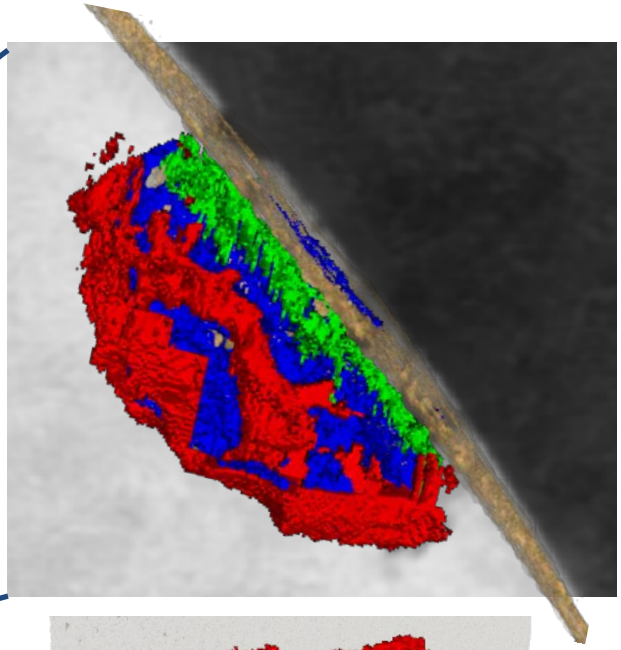

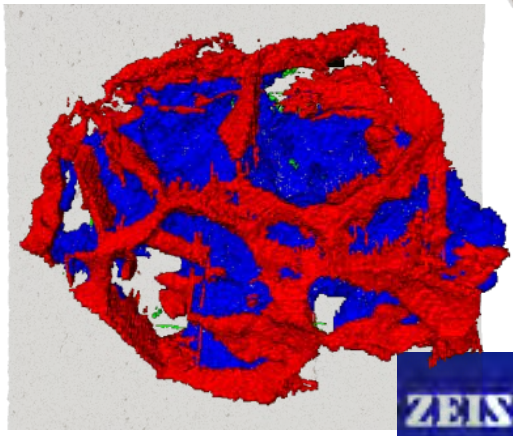

Correlative Tomography: Linking X-ray CT to SEM

Manually register the surface as rendered from X-ray CT to the SEM image to locate periphery of pit obscured by a lacy cover:

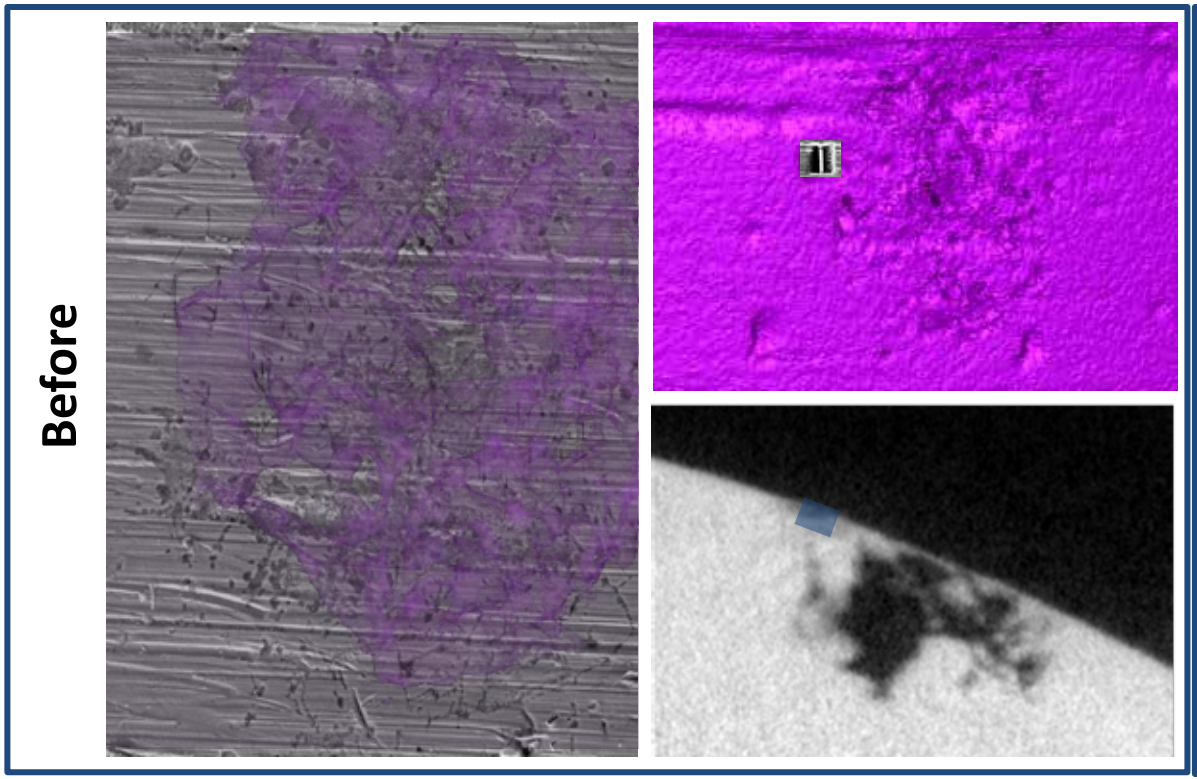

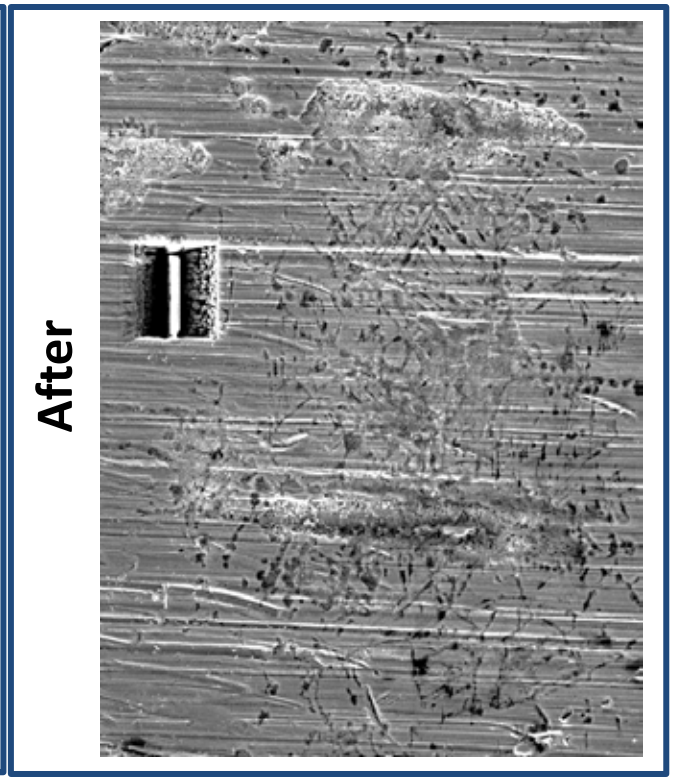

100mm

ZEISS

FEI

Correlative Tomography: FIB-SEM serial sectioning

3D analysis at the nanoscale using Slice and View

- Destructive but very high resolution and SEM imaging reveals contrast from grain boundaries
- Characterize the shape, extent and direction of the corrosion fronts

But we need to understand the crystallography to identify the corrosion fronts….

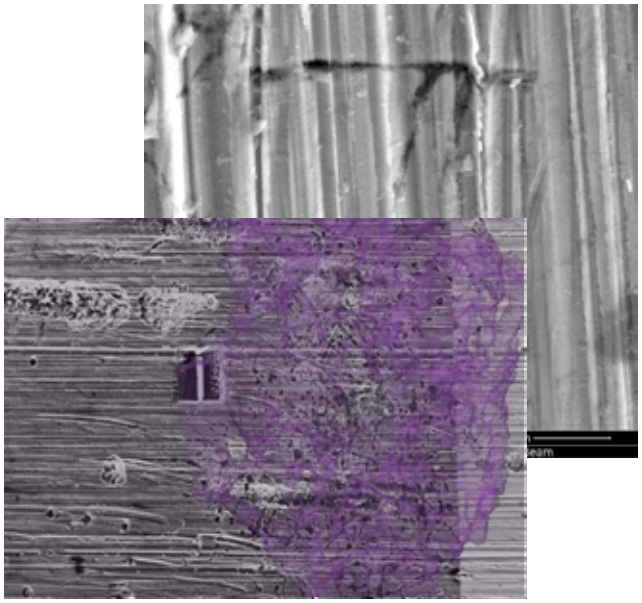

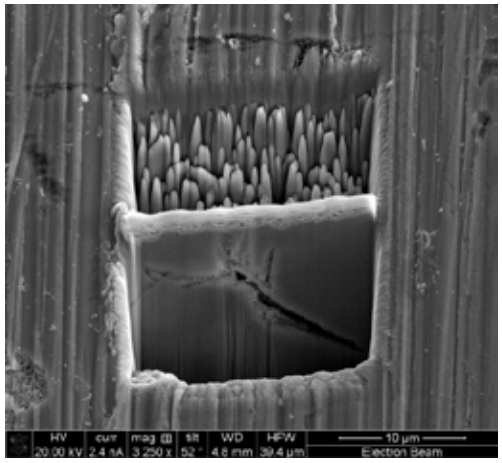

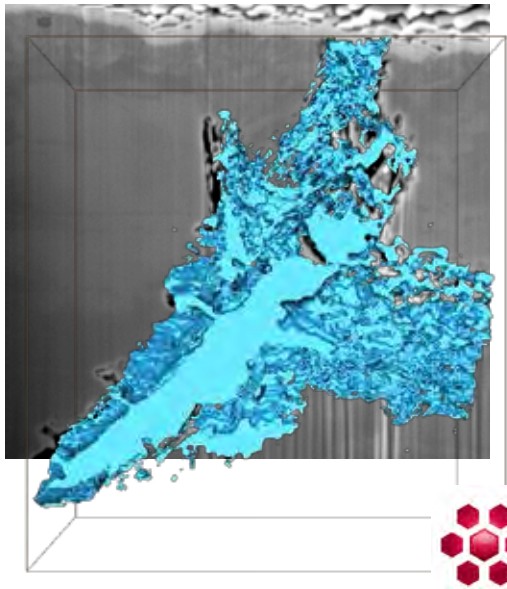

FEI

Connecting Modalities: Crystallography

Electron backscatter diffraction has enabled analysis of the crystallography around the corrosion fronts

- We have identified high angle grain boundaries (A), coincidence site lattice (CSL)(B) and slip bands (C)
- The structural disorder of each of these boundaries appears related to the degree of corrosion

But we need to understand the role of the materials chemistry….

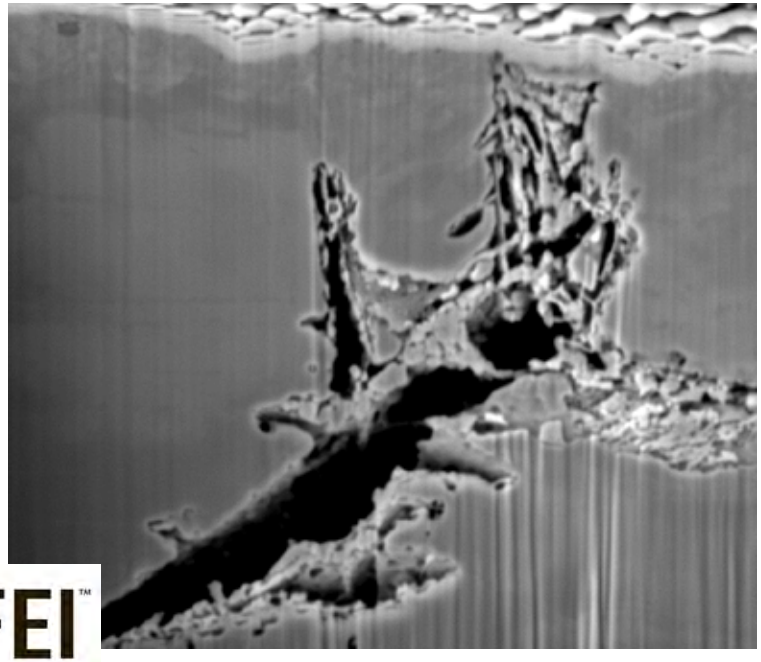

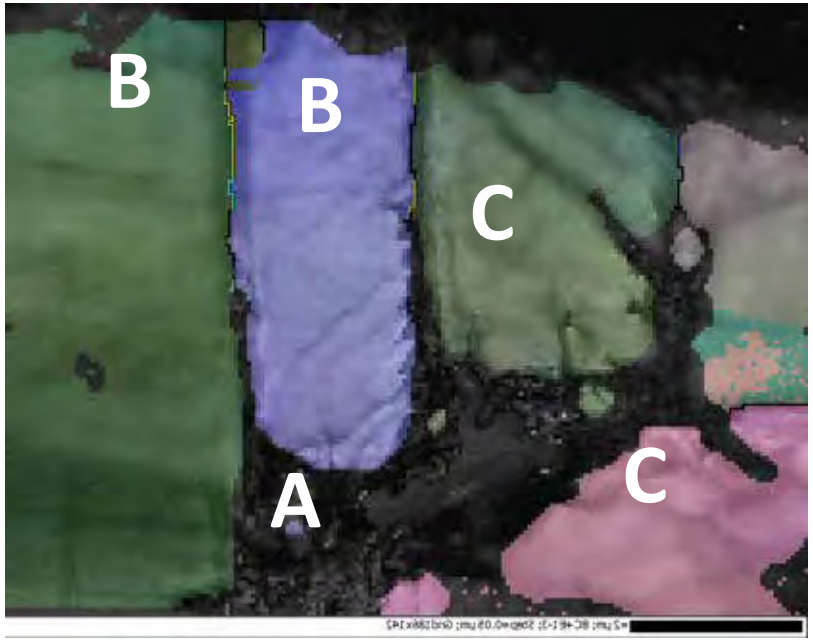

Connecting modalities: Nanoscale Chemical Analysis

Chemical Mapping with Titan ChemiSTEM-EDS

- GB and CSL are associated with chemical segregation
- Slip bands have not yet shown any chemical segregation

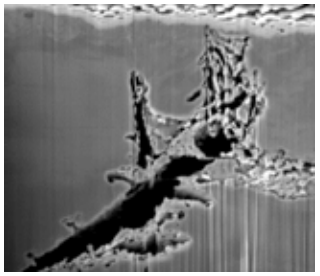

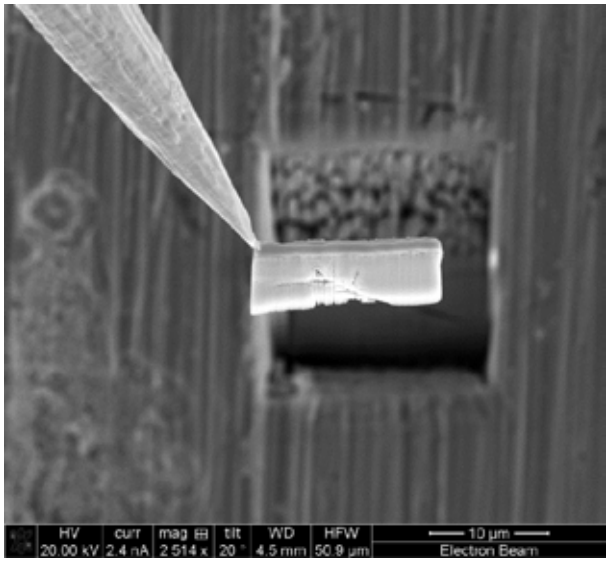

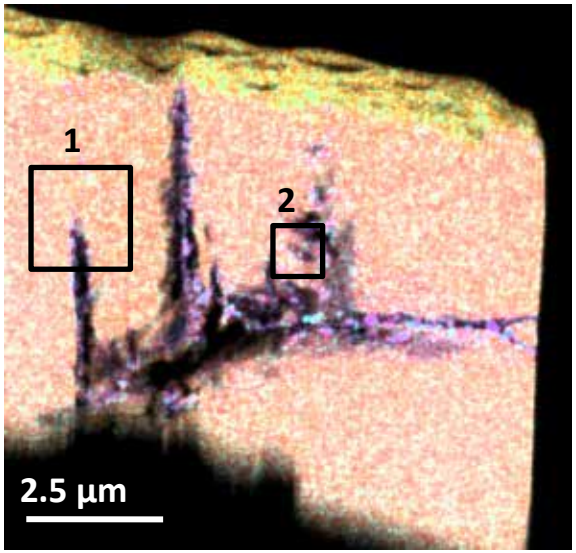

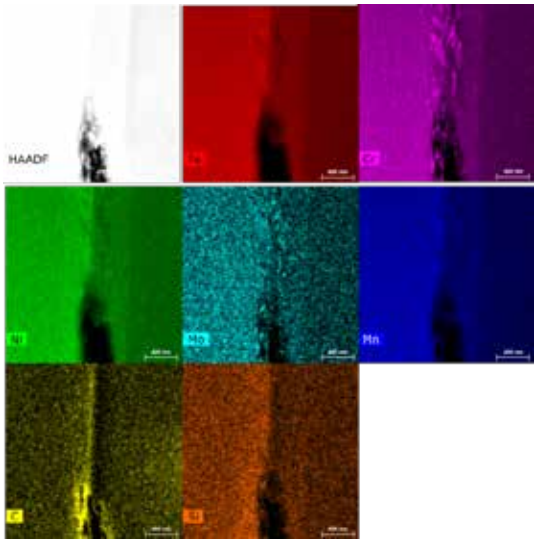

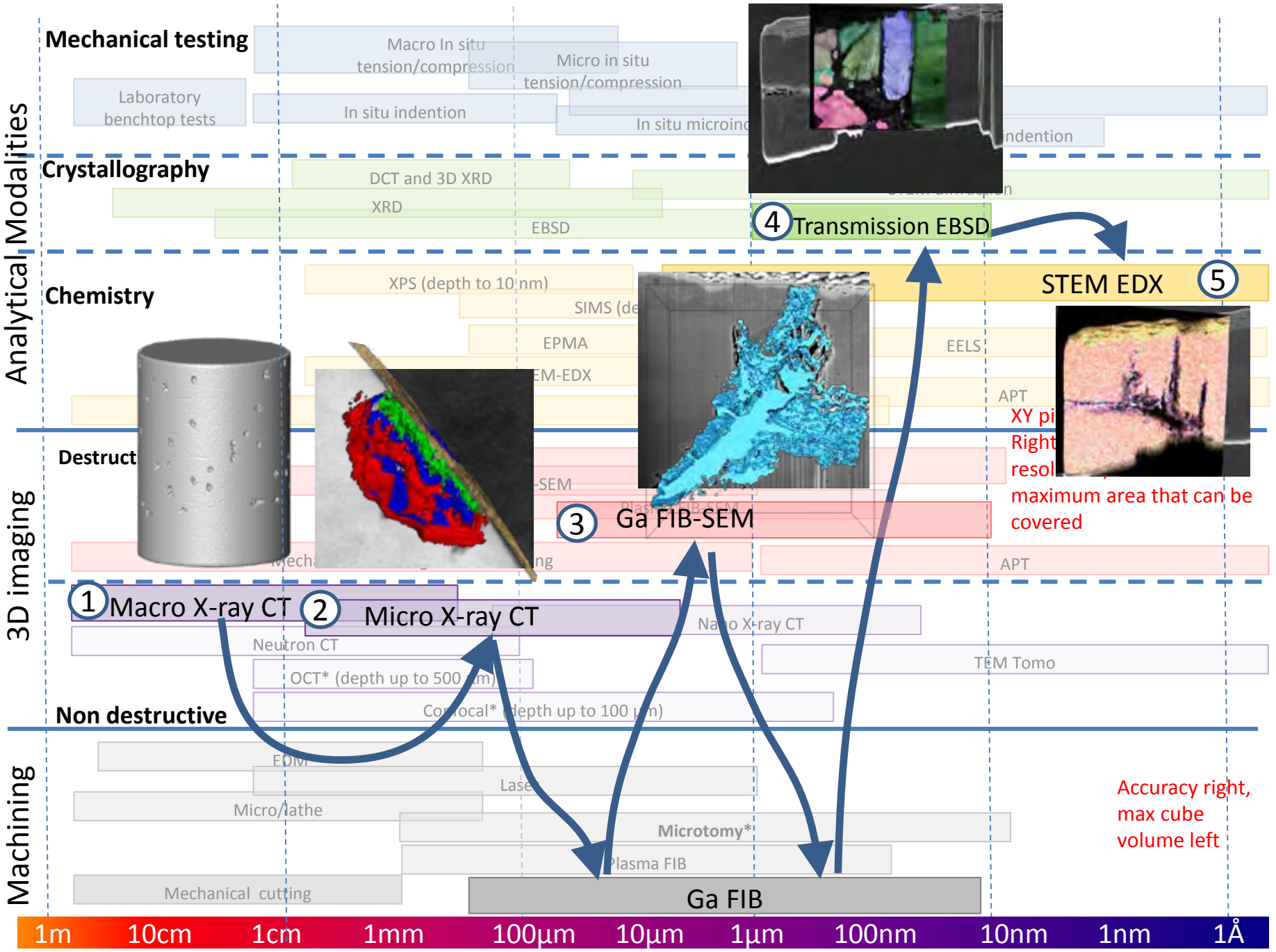
Analytical Modalities
3D imaging
Machining
Mechanical testing
Macro In situ tension/compression
Micro in situ tension/compression
Laboratory benchtop tests
In situ indention
In situ microind
ndention
Crystallography
DCT and 3D XRD
XRD
EBSD
4 Transmission EBSD
Chemistry
XPS (depth to 10 nm)
SIMS (de
EPMA
EM-EDX
EELS
APT
STEM EDX
5
XY pi
Right
resol
maximum area that can be covered
Destruct
-SEM
3 Ga FIB-SEM
ng
APT
1 Macro X-ray CT
2 Micro X-ray CT
Nano X-ray CT
Neutron CT
TEM Tomo
OCT* (depth up to 500 m)
Non destructive
Confocal* (depth up to 100 µm)
EDM
Laser
Micro/lathe
Microtomy*
Plasma FIB
Mechanical cutting
Ga FIB
Accuracy right, max cube volume left
1m
10cm
1cm
1mm
100µm
10µm
1µm
100nm
10nm
1nm
1Å

Correlative Tomography

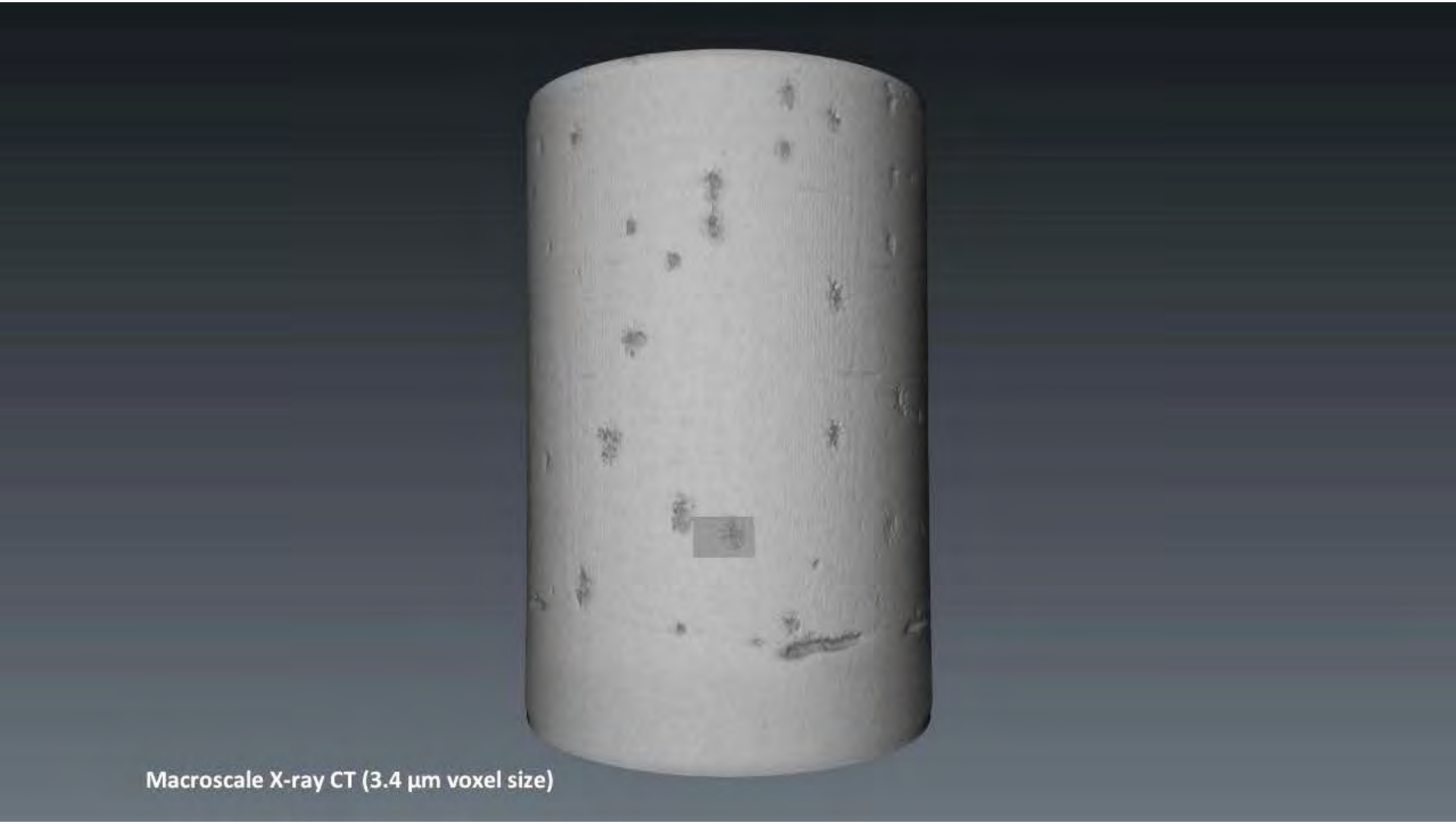

MANCHESTER 1824
The University of Manchester

Summary

- There are a growing number of advanced acquisition and analysis tools available
- Correlative tomography aims to create workflows that effectively connect multiple techniques
- Correlative tomography aims to allow the traversing of multiple time and length scales
- Correlative tomography aims to identify key length scales in an efficient way
- Correlative tomography aims to bring new insights to well-studied systems

Acknowledgements

UoM- Bart Winiarski, Sam MacDonald, Rob Bradley, Tom Slater, Simon Jacques, Chris Egan, Xuekun Lu, Ali Gholinia, Sarah Haigh,, Phil Withers

FEI- Remco Geurts, Ron Kelley, Daniel Lischau

Correlative Tomography TL Burnett et al. Scientific Reports (2014) 4, 04711

Particle movement during the deep penetration of a granular material studied by X-ray microtomography, S.A. McDonald, L.C.R. Schneider, A.C.F. Cocks, P.J. Withers, Scripta Materialia, (2006) Volume 54, Issue 2, January 2006, Pages 191–196

Combining X-ray microtomography and three-dimensional digital volume correlation to track microstructure evolution during sintering of copper powder, S. A. McDonald, P. J. Withers, The Journal of Strain Analysis for Engineering Design March 24, 2014 0309324714527588

Non-destructive mapping of grain orientations in 3D by laboratory X-ray microscopy, S. A. McDonald, P. Reischig, C. Holzner, E. M. Lauridsen, P. J. Withers, A. P. Merkle, and M. Feser Sci Rep. 2015; 5: 14665

3D chemical imaging in the laboratory by hyperspectral X-ray computed tomography. C.K. Egan, S.D.M. Jacques, M.D. Wilson, M.C. Veale, P. Seller, A.M. Beale, R.A.D. Pattrick, P.J. Withers & R.J. Cernik. Scientific Reports (2015) 5, 15979;

Progress towards Five Dimensional Imaging of Functional Materials Under Process Conditions. A.M. Beale, S.D.M. Jacques, E.K. Gibson and M Di Michiel. Coordination Chemistry Reviews (2014) 277-278, 208;

A laboratory system for element specific hyperspectral X-ray imaging. S.D.M. Jacques, C.K. Egan, M.D. Wilson, M.C. Veale, P. Seller and R.J. Cernik. Analyst, (2013) 138, 755-759.